# Spatial Statistics of Tsunami Overland Flow Properties

Luis Montoya, S.M.ASCE[1]; Patrick Lynett, Ph.D., M.ASCE[2]; Hong Kie Thio, Ph.D., M.ASCE[3]; and Wenwen Li, Ph.D., M.ASCE[4]

**Abstract:** Numerical models are a key component of methodologies used to estimate tsunami risk, and model predictions are essential for the development of tsunami hazard assessments (THAs). By better understanding model bias and variability and, if possible, minimizing them, more reliable THAs will result. In this study, the authors compare run-up height, inundation lines, and flow-velocity field measurements between an open-source tsunami model and the method of splitting tsunami (MOST) model predictions in the Sendai Plain in Japan. Run-up elevation and average inundation distance are, in general, overpredicted by the models. However, both models agree relatively well with each other when predicting maximum sea surface elevations and maximum flow velocities. Furthermore, to explore the variability in numerical models, MOST is used to compare predictions from six different grid resolutions (90, 60, 30, 20, 15, and 10 m). Results of this work show that predictions of statistically stable products (run-up, inundation lines, and flow velocities) do not require the use of high-resolution (<30-m) digital elevation maps at this particular location. When predicting run-up heights, inundation lines, and flow velocities, numerical convergence was achieved by using the 30-m resolution grid. In addition, the Froude number variation in overland flow and a MOST sensitivity analysis are presented. Also, run-up height measurements and elevations from the digital elevation map were used to estimate model bias. The results provided in this paper will help provide an understanding of the bias and variability in model predictions and locate possible sources of errors within a model. **DOI: 10.1061/(ASCE)WW.1943-5460.0000363.** 

**Author keywords:** Tsunami; Hazard; Numerical modeling; Run-up; Flow velocity.



## Introduction and Background

On March 11, 2011, a $M_W$ 9.0 earthquake generated a tsunami 130 km off the Japanese coast near Sendai (Mori et al. 2011). This event was one of the worst in Japanese history, killing more than 15,000 people and causing more than $200 billion in damage. Available data show that in some areas, run-up elevations reached 40 m and flow velocities reached more than 14 m/s (Mori et al. 2011; Koshimura and Hayashi 2012). This event raised safety concerns for many coastal communities. Along the Sendai Plain, the tsunami traveled more than 5 km inland with a maximum measured run-up of approximately 9.4 m and at an average of 2.5 m above mean sea level (Mori et al. 2011). The tsunami velocities measured by Koshimura and Hayashi (2012) at different locations on the Sendai Plain ranged from 2 to 8 m/s. Because of the measurements collected during and after the Tohoku event, researchers have a great opportunity to model, study, and understand the nearshore and onshore hydrodynamics of tsunamis. Numerical models are a key component in the development of tsunami hazard assessments (THAs), regardless of whether these assessments are probabilistic or deterministic in nature. When field measurements and model predictions are available, there is an opportunity to better understand model bias and sensitivities, resulting in more accurate and reliable THAs, which will lead to improvement in risk assessment and hazard mitigation in coastal areas susceptible to tsunamis.

In past decades, numerical models that can accurately predict tsunami run-up, inundation, and flow velocity were developed. Because of the surge in state-of-the-art numerical models and their widespread use in this field, there is a need to better understand model predictions and variability for better evacuation and construction planning. In this study, the method of splitting tsunami (MOST) (Titov and Synolakis 1995, 1998) and GeoClaw (LeVeque et al. 2011; Berger et al. 2011) tsunami models are used to compare run-up and flow-velocity results to measured field data. Available field-survey data and video-footage analysis measurements are used to compare model run-up and flow-velocity predictions. Possible sources of error are analyzed and discussed. This study includes detailed comparisons between observations and numerical simulations in Sendai and focuses on the Sendai Plain area.

## Field Measurements and Observations

The field-survey data published by Mori et al. (2011) and the flow-velocity measurements from Koshimura and Hayashi (2012) are used to compare the accuracy and reliability of numerical model predictions. More than 5,300 measurements were recorded by a large group of scientists and researchers. A total of 63 universities and 297 people were involved in this project, which covered 2,000 km of the Japanese coast. In Sendai, the maximum measured run-up elevation was 9.4 m (2011 Tohoku Earthquake Tsunami Joint Survey Group 2011). Only 10% of the run-up measurements were greater than 5 m. For this study, the authors focus on the Sendai Plain (particularly from 38.10°N to 38.28°N). The wave

[1]Ph.D. Student, Research Assistant, Tsunami Research Center, Univ. of Southern California, Los Angeles, CA 90089 (corresponding author). E-mail: lhmontoy@usc.edu

[2]Professor, Tsunami Research Center, Univ. of Southern California, Los Angeles, CA 90089. E-mail: plynett@usc.edu

[3]Principal Seismologist, AECOM, 915 Wilshire Blvd., Los Angeles, CA 90017. E-mail: hong.kie.thio@urs.com

[4]Tsunami Scientist, AECOM, 915 Wilshire Blvd., Los Angeles, CA 90017. E-mail: wenwen.li@aecom.com

Note. This manuscript was submitted on November 24, 2015; approved on June 8, 2016; published online on August 17, 2016. Discussion period open until January 17, 2017; separate discussions must be submitted for individual papers. This paper is part of the ***Journal of Waterway, Port, Coastal, and Ocean Engineering***, © ASCE, ISSN 0733-950X.

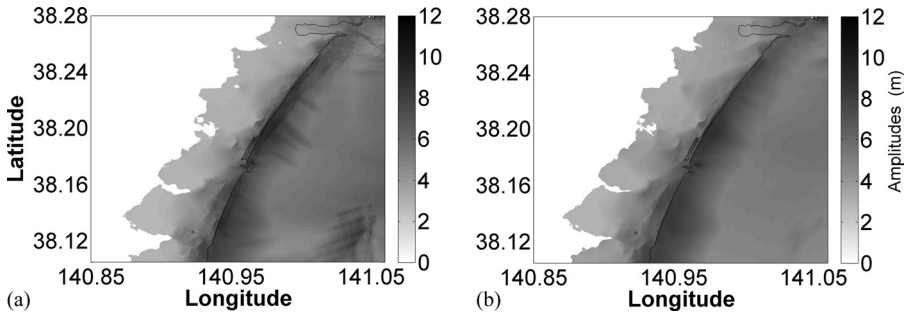


**Fig. 1.** Maximum tsunami amplitudes (in meters) predicted by (a) MOST and (b) GeoClaw for the Sendai Plain

**Table 1.** Field-Data Measurements Not Used in This Study

| Latitude (°N) | Longitude (°E) |
|---|---|
| 38.1725 | 140.9538 |
| 38.1822 | 140.9583 |
| 38.2394 | 140.9533 |
| 38.2718 | 140.9981 |
| 38.2724 | 140.9980 |
| 38.2799 | 141.0506 |
| 38.2799 | 141.0484 |

front at the Sendai Plain during the 2011 tsunami reached more than 5 km inland from the shoreline, and the average was 4.2 km.

Flow-velocity estimates measured by Koshimura and Hayashi (2012) were obtained from a two-dimensional (2D) projective transformation video analysis. One of the two locations at which measurement estimates were made was the Sendai Plain. The video used in the analysis was taken by a Japanese broadcasting company. Flow-velocity estimates were made at four different locations within the Sendai Plain. These locations are at a distance of 1,000 –3,000 m from the coastline. The maximum measured flow speed was 8.0 m/s.

The grids used in this study are from the M7000 digital contoured bathymetric data and the Geographic Information System 10-m digital elevation models. Five nested grids were used in the numerical models. The propagation grid (Grid A) was the coarsest grid at 3 arc-min. Four additional nested grids (1, 20, 4, and 1 arc-sec) were used to cover the area of interest. Also, five additional grids were created (3, 2, 0.67, 0.50, and 0.33 arc-sec) by interpolating the 4- and 1-arc-sec grid. These grids were used to analyze convergence and variability within the MOST model predictions. All the grids are referenced to mean sea level vertical data and to the World Geodetic System of 1984 (WGS 84) horizontal data.

## Tsunami Modeling

The MOST model was developed as part of the Early Detection and Forecast of Tsunami project and introduced by Titov and Synolakis (1995, 1998). This model is currently used by the National Oceanic and Atmospheric Administration for propagation and inundation forecasting (Titov 2009). The MOST model has been validated and tested successfully in various studies (Synolakis et al. 2007; Titov and Synolakis 1998; Titov and Gonzalez 1997). Wei et al. (2013) modeled the 2011 Tohoku tsunami with MOST and presented a detailed analysis of run-up height and inundation along the Japanese coast. MOST solves the $2+1$ nonlinear shallow-water equations

$$h_t + (uh)_x + (vh)_y = 0 \tag{1}$$

$$u_t + uu_x + vu_y + gh_x = gd_x - Du \tag{2}$$

$$v_t + uv_x + vv_y + gh_y = gd_y - Dv \tag{3}$$

where $\eta(x,y,t)$ = wave amplitude; $d$ = water depth; $h(x,y,t) = \eta(x,y,t) + d(x,y,t)$; $u(x,y,t)$ and $v(x,y,t)$ = depth-averaged velocities; and $D(h,u,v)$ = drag coefficient computed by Eq. (4)

$$D(h,u,v) = n^2 g h^{-4/3}\sqrt{u^2+v^2} \tag{4}$$

Run-up and inundation were performed only in the higher-resolution grids (3, 2, 1, 0.67, 0.5, and 0.4 arc-sec or approximately 90, 60, 30, 20, 15, and 10 m, respectively). To evaluate the MOST model sensitivity to the Manning coefficient, three different values were used for the simulations, $n$ = 0.025, 0.030, and 0.035. For a detailed description of MOST, refer to Titov and Synolakis (1995, 1998).

GeoClaw (LeVeque et al. 2011), developed originally by George in 2004 (George 2004), is an open-source tsunami model approved by the U.S. National Tsunami Hazard Mitigation Program (LeVeque 1997, 2002). It has been validated by comparing real and artificial data (run-up, inundation, and flow-velocity data) with model results (Arcos and LeVeque 2015; Gonzalez et al. 2011; LeVeque et al. 2011; Berger et al. 2011; George 2008; LeVeque and George 2008). GeoClaw uses finite volume methods to solve 2D nonlinear shallow-water equations in conservative form

$$h_t + (uh)_x + (vh)_y = 0 \tag{5}$$

$$(hu)_t + \left(hu^2 + \frac{1}{2}gh^2\right)_x + (huv)_y = -ghB_x - Dhu \tag{6}$$

$$(hv)_t + (huv)_x + \left(hv^2 + \frac{1}{2}gh^2\right)_y = -ghB_y - Dhv \tag{7}$$

where $h(x,y,t)$ = fluid depth; $u(x,y,t)$ and $v(x,y,t)$ = depth-averaged velocities; $B(x,y,t)$ = topography or bathymetry; and $D(h,u,v)$ = drag coefficient computed by Eq. (4) with the Manning coefficient, $n$ = 0.025, constant throughout the grid. For a detailed description of GeoClaw, refer to LeVeque et al. (2011) and Berger et al. (2011).

For this study, two modifications were made to the GeoClaw code to perform the tsunami simulation. First, the code was modified to use fixed grids instead adaptive mesh refinement. Then, the modified code uses the generic mapping tool network common data form files as inputs and outputs. Most of the parameters are the

same as those used by MacInnes et al. (2013) except for the minimum allowable water depth (geo_data.dry_tolerance), set to 0.01 m, and maximum depth at which bottom friction is included in the calculations (geo_data.friction_depth), set to 100 m.

The initial condition used in both models is an initial sea-surface deformation based on Yokota et al. (2011). This source model was created by carrying out a quadruple joint inversion of the strong motion, teleseismic, geodetic, and tsunami data sets. The resulting model has a maximum coseismic slip of approximately 35 m and a seismic moment of $4.2 \times 10^{22}$ Nm, which yields a $M_W$ of 9.0.

## Results and Discussion

### *Intermodel Comparison*

A 30-m-resolution grid was used for the intermodel comparison analysis. Also, as was mentioned previously, three different Manning values ($n$ = 0.025, 0.030, and 0.035) were used in MOST to evaluate its sensitivity to predict run-up elevations and overland flow velocities. Fig. 1 shows the maximum free-surface elevation during the Tohoku tsunami event for MOST and GeoClaw. Both models predict that higher free-surface elevations occur at the central part of the Sendai Plain, around 38.2°N 140.975°E, with maximum wave amplitudes ranging from 8 to 12 m. Both models agree relatively well with each other when predicting sea-surface elevation near the shoreline, but MOST yields slightly higher predictions.

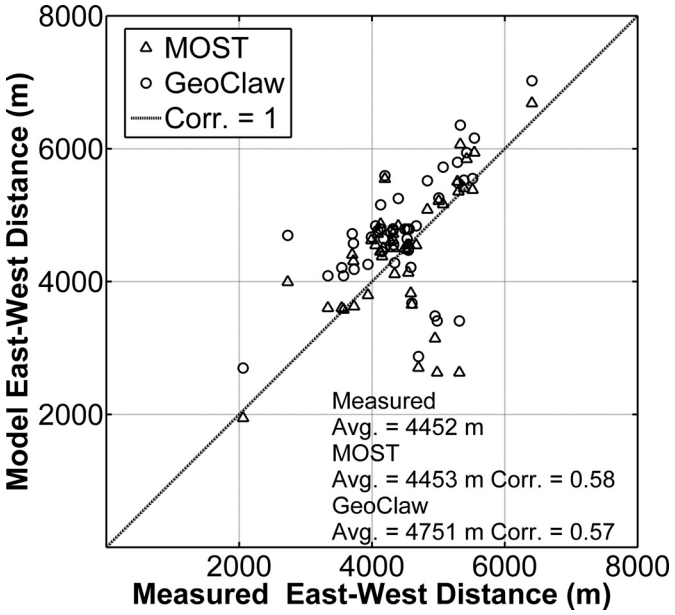


**Fig. 2.** Comparison between measured east-west distances and model-predicted distances in the Sendai Plain (Note: Corr. = correlation coefficient)

For consistency purposes, 7 run-up measurements from the field data were removed from the analysis (Table 1). These run-up measurements were located very close to the shoreline and led to an irregular inundation line when combined with the other run-up points. A total of 46 run-up measurements were used from the Sendai Plain in this analysis. Fig. 2 presents the east-west distances measured versus the east-west distances predicted by both models. The average distances are 4,452, 4,752, and 4,453 m for the measured data, GeoClaw, and MOST respectively. The calculated relative accuracy for MOST is $1.02 \pm 0.18$, whereas for GeoClaw it is $1.08 \pm 0.19$ (where $1.00 \pm 0.00$ would be perfect agreement). In general, both models overpredict the east-west distances in the Sendai Plain, but GeoClaw makes slightly higher predictions than MOST.

Fig. 3(a) shows the field-data run-up measurements and the predicted run-ups according to both models. The average run-up from the 46 field-data measurements is 1.89 m, with a standard deviation of 0.70 m, whereas the average run-ups calculated by MOST and GeoClaw are 3.01 and 3.34 m, respectively. Thus, much of the model run-up results lay approximately 2 to 3 standard deviations away from the mean of the field data. The run-up standard deviations for MOST and GeoClaw are 0.16 and 0.33 m, respectively. Fig. 3(b) shows the inundation line predicted by both models and the field-data run-up height measurements at the Sendai Plain (38.10°N to 38.28°N). Both models provide a reasonably accurate prediction of the inundation line. This would seem to indicate an inconsistency, in that the inundation line is well predicted, but the run-up elevation is not; this point will be addressed later in this section.

Fig. 4 presents the variability of run-up and inundation-line predictions using different $n$ values. It can be seen that run-ups decrease with higher $n$ values, therefore reducing the models' error. The Sendia's average run-up calculated by MOST are 2.59 and 2.51 m using $n$ values of 0.030 and 0.035, respectively. It is very interesting to note that there is a much higher difference in the run-up and inundation-line predictions when increasing the $n$ value from 0.025 to 0.030 than from 0.030 to 0.035, which would indicate that accurate run-up elevation predictions require both high precision and accuracy in bottom friction in this area.

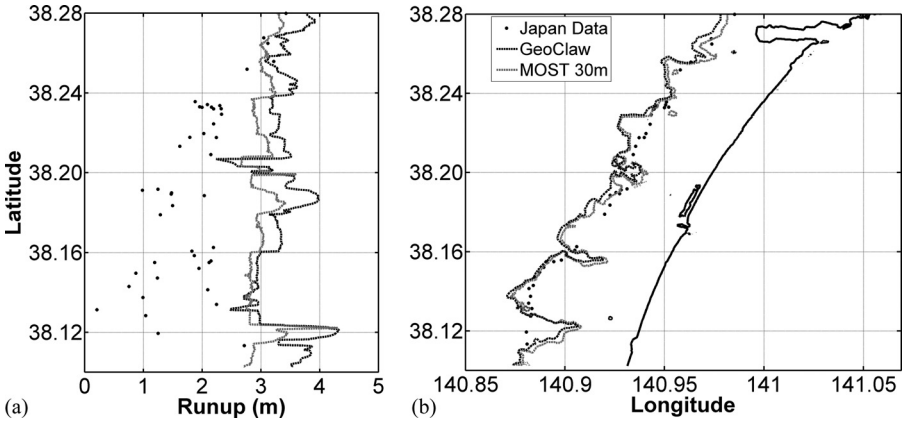


**Fig. 3.** Comparison of (a) run-up height measurements and (b) inundation-line data with MOST and GeoClaw predictions during the 2011 Tohoku event in the Sendai Plain (Manning $n$ = 0.025)

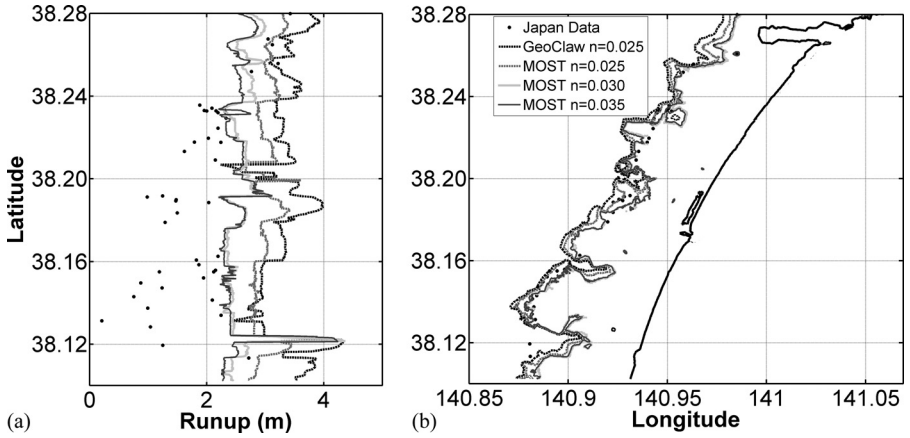


**Fig. 4.** (a) Comparison of run-up height measurements and (b) inundation-line data with MOST predictions using different Manning *n* values during the 2011 Tohoku event in the Sendai Plain

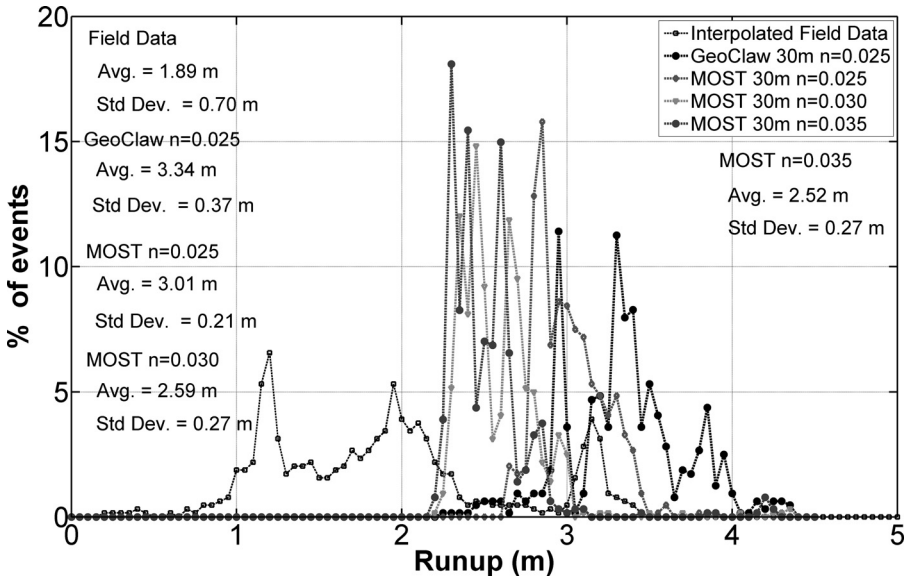


**Fig. 5.** Comparison of the run-up height distributions between the interpolated field data and the MOST and GeoClaw models; the distributions use a run-up interval spacing of 0.05 m

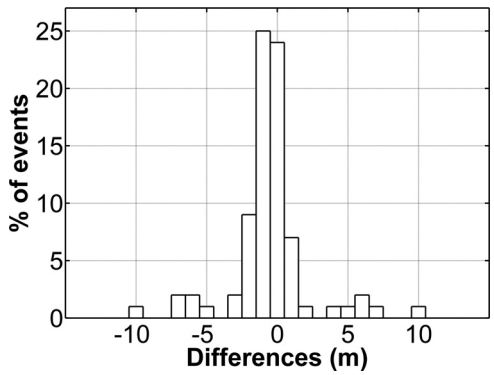


**Fig. 6.** Estimated differences between field-data run-up heights and the topographic elevations from the numerical grid at the location of the run-up measurement

Fig. 5 shows the distributions of the run-up height from the field data and the models. This normalized histogram, and all histograms presented in this paper, were generated using all relevant field or modeled data between 38.10°N and 38.28°N along the Sendia plain. The distribution uses a run-up interval spacing (histogram bin width) of 0.05 m. The model distributions have a similar shape, with means within 10% of each other, but it can be clearly noted that they overestimate the observed run-up. By using different higher *n* values, the shape of the distributions remains similar but the peaks tend to move left, decreasing the error of the MOST model predictions. To further analyze the run-up predicted by both models, the authors compared the field-data run-up height measurements with the elevation from the numerical topographic grid at the location of the run-up measurements. The Sendai 30-m resolution topography was used in this analysis. Fig. 6 presents a histogram of the estimated differences and shows that most of the differences range between −3 m and −1 m. This indicates that there is some

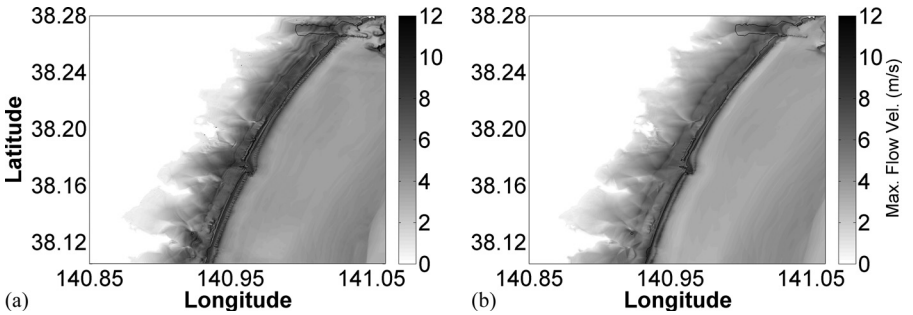


**Fig. 7.** Maximum flow velocities predicted by (a) MOST and (b) GeoClaw

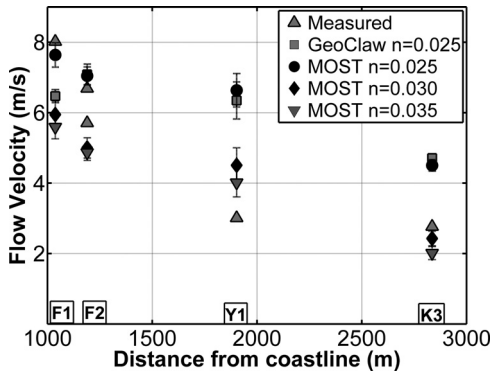


**Fig. 8.** Comparison of maximum flow velocities at the Sendai Plain between Koshimura and Hayashi (2012) measurements, GeoClaw predictions, and MOST predictions using $n$ = 0.025, 0.030, and 0.055; the vertical bars provide the standard deviation of the predictions in the measurement window (Note: At F2, two measurements were taken)

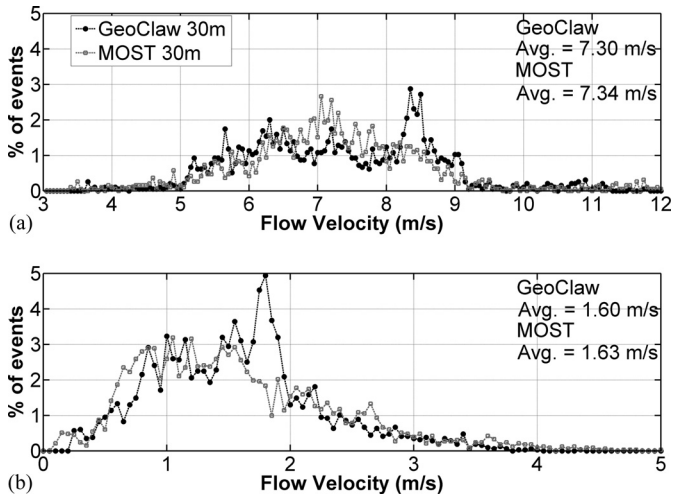


**Fig. 9.** Comparison between (a) GeoClaw and MOST distributions of maximum shoreline flow velocities and (b) 1-m-depth maximum flow velocities at the Sendai Plain; the distributions use a velocity interval spacing of 0.05 m/s

error in the topography, one that cannot be attributed simply to a datum inconsistency caused by the spread of the histogram. The differences between run-up elevations and topographic grid elevations would also indicate that it should not be possible for a model to agree with both the inundation line and the run-up elevation when using these Geographic Information System topography data. This inconsistency is a result of the fact that run-up measurements include small-scale local topography, whereas the grid does not (e.g., topography features with length scales smaller than the topographic resolution). Such errors are particularly significant for flat coastal areas such as the Sendai Plain.

In addition to flow depths, tsunami flow velocities have to be analyzed for the tsunami hazard at a particular location to be understood. For example, Synolakis (2004) stated that currents are more destructive than wave height amplitudes during many tsunami events. Lynett et al. (2012, 2014) showed the effects of tsunami-induced currents in harbors. Fig. 7 presents the maximum flow velocities predicted by MOST and GeoClaw in the Sendai Plain. Both models agree on their predictions and locations of high flow velocities. They also both show a rather complex profile of overland flow velocity, with a number of local maxima. These local maxima are a result of topographic features and properties of the incident wave form.

Koshimura and Hayashi (2012) measured the tsunami flow velocities at 4 different locations in the Sendai Plain. Fig. 8 shows the modeled tsunami flow velocities and the field measurements at these locations. When using an $n$ value of 0.025, both models underpredict the flow velocity at F1, which is close to the coastline, and overpredict it at F2, Y1, and K3, which are further inland. Fig. 8 also shows the modeled flow velocities predicted by MOST using different $n$ values. It can be seen that the error increases near the shoreline (less than 1,500 m) when a higher value of $n$ is used. Farther inland, the error decreases and the predicted velocities move closer to the measured velocity but still overpredict at Y1 and underpredict at K3. Using higher values of Manning coefficients ($n$ = 0.030 or 0.035) can be suggested when analyzing overland flow properties far from the coastline (>1,500 m) to decrease error in the predictions. Both models use uniform Manning $n$ coefficients throughout the grid, which might be a reason why the

**Table 2.** Simulation Run Times (for 10 h of Physical Time) and Relevant Information for Each Grid Resolution

| Grid resolution (m) | Run time (min) | No. of threads used | $nx$ | $ny$ | Time step (s) |
|---|---|---|---|---|---|
| 90 | 20 | 8 | 415 | 355 | 0.5 |
| 60 | 41 | 8 | 623 | 533 | 0.5 |
| 30 | 190 | 8 | 1,244 | 1,064 | 0.5 |
| 20 | 431 | 8 | 1,607 | 1,595 | 0.5 |
| 15 | 750 | 8 | 2,142 | 2,126 | 0.5 |
| 10 | 1713 | 8 | 3,729 | 3,189 | 0.25 |

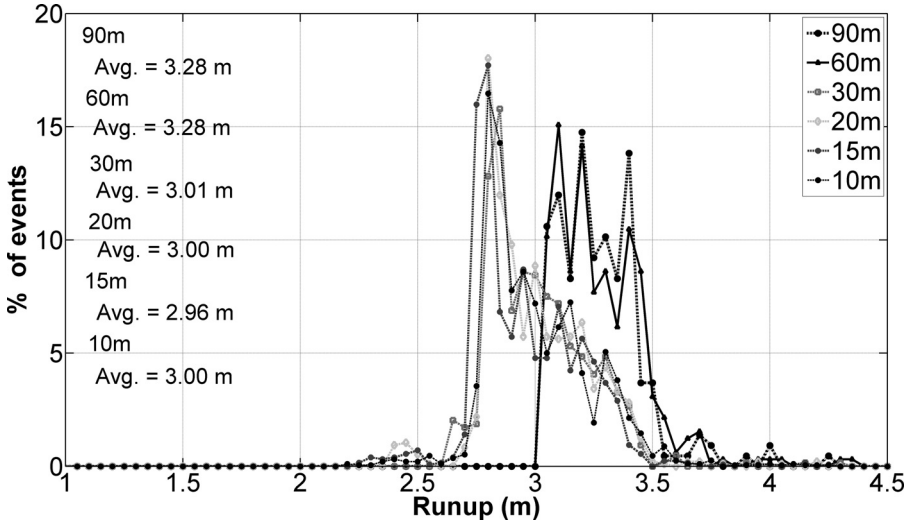


**Fig. 10.** Comparison of the run-up height distributions between the six different grid resolutions using MOST; the distributions use a run-up interval spacing of 0.05 m

models overpredict or underpredict farther inland. This observation is an indication that spatially variable bottom roughness is likely necessary to capture local flow speeds; such an implementation is certainty viable but would require spatial maps of ground properties, which could be used to construct friction factor maps. Furthermore, the ground properties will change in time after interaction with the tsunami (i.e., erosion, flattening of vegetation), leading to a substantial modeling challenge. Other reasons for a numerical model to overestimate or underestimate flow-velocity measurements include complex and unresolved bathymetry/topography, improper friction coefficients, no inclusion of tides, and numerical dispersion and dissipation errors.

Fig. 9 shows a comparison of the distributions of modeled maximum shoreline flow velocity and flow velocity at the 1-m inland flow depth. The distributions use a flow-velocity interval spacing of 0.05 m/s. These two locations are meant to represent limits of the overland flow area, one comparison at the shoreline and another near the inundation limit, but still at a significant flow depth. Because there are no available data for these locations, it is very difficult to assess the model's accuracy. Many of the model velocity predictions at the shoreline are between 5 and 9 m/s, with means of 7.30 and 7.34 m/s for GeoClaw and MOST, respectively. The shapes of the shoreline flow-velocity distributions tend to agree well with small differences in their means. Fig. 9(b) shows that both models agree well when predicting the maximum flow velocities at the 1-m flow depth. The peak of the GeoClaw distribution is located around 1.63 m/s, with an average of 1.60 m/s, whereas the peak for MOST is located around 1.20 m/s, with an average of 1.63 m/s.

### *MOST Model Variability*

Unquantified variabilities within a model can lead to unknown errors in a THA. In this section, the authors use MOST to further explore and understand the possible sources of error within a model. For this part of the analysis, six inundation grids (3, 2, 1, 0.67, 0.50, and 0.33 arc-sec) were used to compare inundation, run-up, and velocity predictions made by the MOST model. As was mentioned previously, finer grids were created by interpolating the 4- and 1-arc-sec topography data. Overall run times for each resolution are presented in Table 2. All the simulations were performed for a physical time of 10 h. The CPU used was an AMD Opteron 6140 running at

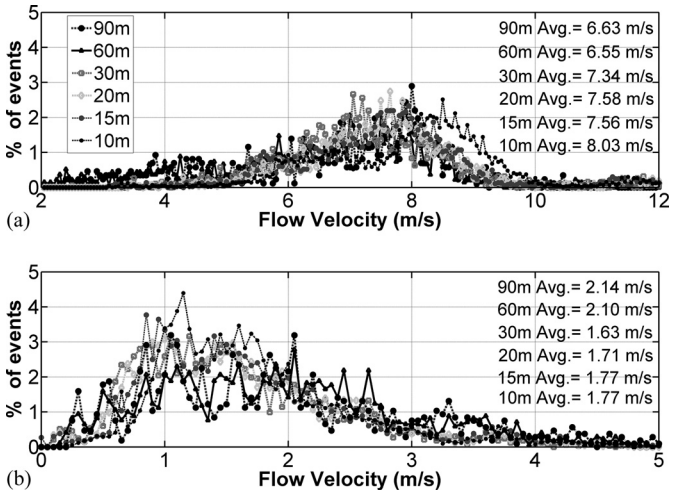


**Fig. 11.** Comparison of (a) the maximum shoreline flow-velocity distributions and (b) 1-m-depth maximum flow-velocity distributions between the six different grid resolutions using MOST; the distributions use a flow-velocity interval spacing of 0.05 m/s

2.6 GHz. Run times are increased by almost a factor of 4 when the grid resolution is increased by a factor of 2 (i.e., from 30 to 15 m). Fig. 10 shows a distribution of the run-up height calculations from the different grids. Both run-up and inundation-line predictions numerically converge within the tested grid sizes. There are small deviations in the inundation-line and run-up calculations when using different grid resolutions (30–10 m). In this case, it would seem reasonable to conclude that there is no need to use inundation grids finer than 30 m when calculating run-up and inundation lines.

Fig. 11 shows a comparison of maximum shoreline flow-velocity distributions and 1-m-flow-depth maximum-velocity distributions for the different grid resolutions. Averages for shoreline velocities are approximately 7.50 m/s, and for 1-m flow depth, the velocities are approximately 1.70 m/s. Although there appears to be numerical convergence between the 30-, 20-, and 15-m-resolution simulations at the shoreline, the 10-m-resolution grid diverges, with an average maximum velocity of 8.03 m/s. Although this divergence is relatively small with a change of 7% in mean values between the 15- and 10-m results,

it is a difference that is not easy to reconcile. From inspection of the results, this variance between the 15- and 10-m results seems to be driven by a difference in the prediction of the steep front of the incoming bore, and with the understanding that breaking in this model is controlled through numerical dissipation, it is difficult to assess whether this variance is physical (better resolution of the process) or numerical (different numerical errors). Stable numerical results were not achievable for grid sizes less than 10 m. Such a divergence with finer resolutions is not found at the inland location.

Fig. 12 shows the calculated mean flow velocity at six different flow depths (where 6 m corresponds approximately to the shoreline). It is very interesting to note that the mean speeds, with the exception of the 90- and 60-m resolution results, converge at a flow depth of 1 m. Also, the greatest increase in flow velocity between flow depths was found to be from 2 to 3 m with an average increase of 2.69 m/s for the tested grids. The Froude number, $V/\sqrt{gh}$, where $V$ = magnitude of the overland flow velocity and $h$ = overland flow depth, is commonly used to constrain flow depth and speed for tsunamis when tracing deposits. Fig. 12 presents the variability of the Froude number at the Sendai Plain and shows an irregular Froude-number profile. The Froude number is very near 1 at the shoreline, greater than 1 (supercritical flow) at flow depths of 3–4 m, and less than 1 (subcritical flow) at flow depths of 1–2 m.

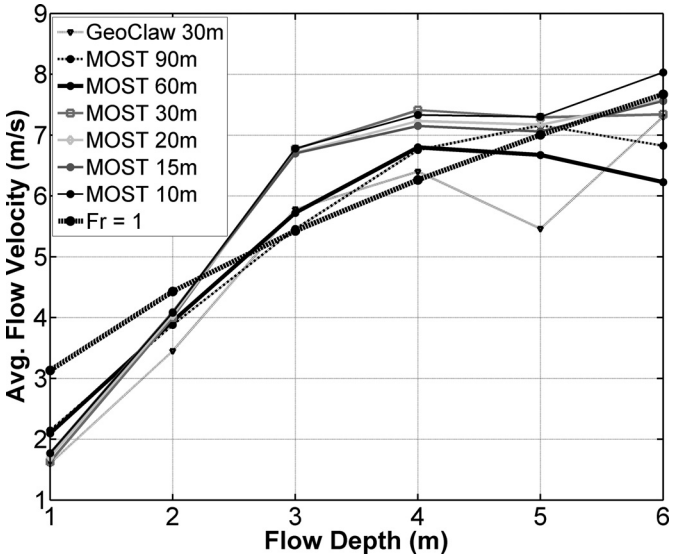


**Fig. 12.** Mean flow velocities at different flow depths; the 6-m flow depth corresponds approximately to the shoreline (Note: The thick black line = calculated mean flow velocities using a Froude number of 1)

It is reasonable to expect a steady decrease in velocity, if using the assumption of a simple beach, as the wave front makes its way inland; however, the simulation results provided in Fig. 13(a) show otherwise. Between 400 and 1,200 m inland, maximum velocities (again, the mean of the maximum velocities across the studied Sendia Plain) appear to be constant. After analyzing the numerical output, the authors observe that small bathymetry/topography features can cause large changes in predicted flow velocities and produce secondary peaks. Further inland, results from MOST show a steady decline in velocity from 1,200 to 2,800 m with a negative slope of approximately –0.002 for all grid resolutions. Peak flow velocities fluctuate from 6 to 17 m/s and standard deviations from 0.9 to 1.7 m/s. Finally, it is interesting to note that Fig. 13(b) shows abrupt changes in the peak flow velocities near the shoreline. These results agree with the fact that when a breaking bore hits the shoreline, the front suddenly accelerates; the first data point shows this sudden acceleration. This phenomenon was investigated by Synolakis (1987).

## Conclusions

This study presents a comparison between field data and model predictions of the 2011 Tohoku tsunami. In general, the run-up

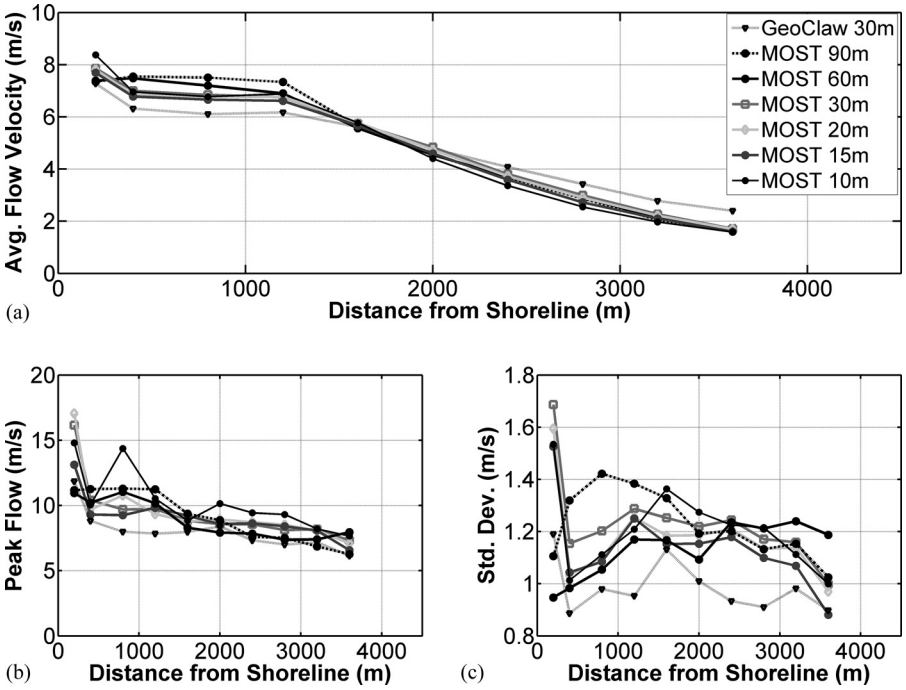


**Fig. 13.** Inland maximum flow velocities across shore in the Sendai Plain: (a) comparison of average flow velocities between GeoClaw and the six different grid resolutions using MOST; (b) comparison of peak flow velocities; (c) comparison of standard deviations

elevation was overpredicted by the models. In contrast, the inundation lines predicted by the models were in good agreement with those observed, and this inconsistency can be attributed to errors in the topographical data. By comparing observed run-up elevation measurements to DEM elevations at the same location, the topography bias ranged from −3 to −1 m. This bias is very significant for this particular location, because the Sendai Plain is, of course, relatively flat. Thus, with this topography, it should not be possible to get both the run-up elevation and inundation line correct. For intermodel agreement, both numerical models, MOST and GeoClaw, agree relatively well with each other when predicting maximum sea-surface elevations and maximum velocities, with MOST yielding slightly higher predictions for both. Also, it is important to note that the two models predict similar maximum velocities at the shoreline (Fig. 9), which is typically the most important place to do so. The MOST sensitivity analysis to the Manning coefficient revealed that higher $n$ values yield more precise run-up elevations. The error for overland flow velocity increased at distances less than 1,500 m and greatly decreased at larger distances.

When predicting run-up heights and inundation lines with MOST, numerical convergence was achieved by using the 30-m-resolution inundation grid. It can be suggested that grids finer than 30-m resolution are not necessary when calculating these products at this particular location. In general, when trying to simulate velocities, it is recommended to use higher-resolution topography because small local changes in bathymetry/topography can cause similarly large local changes in the speed. Predictions of overland flow showed that the Froude number varies at different flow depths. At flow depths of 3–4 m, the flow is considered supercritical, which indicates that speed would increase in the presence of buildings or structures. It was expected that the maximum flow velocity would decrease as the wave makes its way inland, but this pattern was not obvious between the 400- and 1,200-m contour lines, because complexities in the topography and flooding waves obscure this idealized expectation. Finally, it is suggested that an uncertainty analysis, such as a probabilistic description of input parameters leading to probabilistic output, would provide a more complete understanding of the distribution of possible model predictions.

## References


2011 Tohoku Earthquake Tsunami Joint Survey Group. (2011). "Field survey of 2011 Tohoku earthquake tsunami by the Nationwide Tsunami Survey." *Jpn. Soc. Civ. Eng.*

Arcos, M. E. M., and LeVeque, R. J. (2015). "Validating velocities in the GeoClaw tsunami model using observations near Hawaii from the 2011 Tohoku tsunami." *Pure Appl. Geophys.*, 172(3–4), 849–867.

Berger, M. J., George, D. L., LeVeque, R. J, and Mandli, K. T. (2011). "The GeoClaw software for depth-averaged flows with adaptive refinement." *Adv. Water Res.*, 34(9), 1195–1206.

George, D. L. (2004). "Numerical approximation of the nonlinear shallow water equations: A Godunov-type scheme." Master's thesis, Univ. of Washington, Seattle.

George, D. L. (2008). "Augmented Riemann solvers for the shallow water equations over variable topography with steady states and inundation." *J. Comput. Phys*, 227(6), 3089–3113.

Gonzalez, F. I., LeVeque, R. J., Chamberlain, P., Hirai, B., Varkovitzky, J., and George, D. L. (2011). "GeoClaw results for the NTHMP tsunami benchmark problems." *Proceedings and results of the 2011 NTHMP model benchmarking workshop, NOAA Special Report*, U.S. Dept. of Commerce/NOAA/NTHMP, Boulder, CO.

Koshimura, S., and Hayashi, S. (2012). "Tsunami flow measurement using the video recorded during the 2011 Tohoku tsunami attack." *Proc., Geoscience and Remote Sensing Symp. (IGARSS)*, Vol. 22–27, IEEE, New York, 6693–6696.

LeVeque, R. J. (1997). "Wave propagation algorithms for multidimensional hyperbolic systems." *J. Comput. Phys.*, 131(2), 327–353.

LeVeque, R. J. (2002). *Finite volume methods for hyperbolic problems*, Cambridge University Press, Cambridge, England.

LeVeque, R. J., and George, D. L. (2008). "High-resolution finite volume methods for the shallow water equations with bathymetry and dry states." *Advances in coastal and ocean engineering, Vol. 10: Advanced numerical models for simulating tsunami waves and runup,* P. L. Liu, C. Synolakis, and H. Yeh, eds., World Scientific, Singapore, 43–73.

LeVeque, R. J., George, D. L., and Berger, M. J. (2011). "Tsunami modelling with adaptively refined finite volume methods." *Acta Numerica*, 211–289.

Lynett, P., Borrero, J., Son, S., Wilson, R., and Miller, K. (2014). "Assessment of the tsunami-induced current hazard." *Geophys. Res. Lett.*, 41(6), 2048–2055.

Lynett, P., Borrero, J., Weiss, R., Son, S., Greer, D., and Renteria, W. (2012). "Observations and modeling of tsunami-induced currents in ports and harbors." *Earth Planet. Sci. Lett.*, 327–328, 68–74.

MacInnes, B. T., Gusman, A. R., LeVeque, R. J., and Tanioka, Y. (2013). "Comparison of earthquake source models for the 2011 Tohoku event using tsunami simulations and near-field observations." *Bull. Seismol. Soc. Am.*, 103(2B), 1256–1274.

Mori, N., Takahashi, T., Yasuda, T., and Yanagisawa, H. (2011). "Survey of 2011 Tohoku earthquake tsunami inundation and run-up." *Geophys. Res. Lett.*, 38(7), L00G14.

Synolakis, C. E. (1987). "The runup of solitary waves." *J. Fluid Mech.*, 185(1), 523–545.

Synolakis, C. E. (2004). "Tsunami and seiche." *Earth-quake engineering handbook*, W. F. Chen, and C. Scawthorn, Eds., CRC Press, Boca Raton, FL, 9-1–9-90.

Synolakis, C. E., Berbabrd, E. N., Titov, V. V., Kanoglu, U., and Gonzalez, F. I. (2007). "Standards, criteria, and procedures for NOAA evaluation of tsunami numerical models." *NOAA Tech. Memo OAR PMEL-135,* NOAA/Pacific Marine Environmental Laboratory, Seattle, WA.

Titov, V. V. (2009). "In the sea." *Tsunamis, Vol. 15: Tsunami forecasting*, Harvard University Press, Cambridge, MA, 371–400.

Titov, V. V., and Gonzalez, F. I. (1997). "Implementation and testing of the method of splitting tsunami (MOST) model." *Technical Rep., NOAA Tech. Memo ERLPMEL-112 (PB98-122773)*, NOAA/Pacific Marine Environmental Laboratory, Seattle, WA.

Titov, V. V., and Synolakis, C. E. (1995). "Modeling of breaking and nonbreaking long wave evolution and runup using VTSC-2." *J. Waterw. Port Coastal Ocean Eng.*, 10.1061/(ASCE)0733-950X(1995)121:6(308), 308–316.

Titov, V. V., and Synolakis, C. E. (1998). "Numerical modeling of tidal wave runup." *J. Waterw. Port Coastal Ocean Eng.*, 10.1061/(ASCE)0733-950X(1998)124:4(157), 157–171.

Wei, Y., Chamberlin, C., Titov, V. V., Tang, L., and Bernanrd, E. N. (2013). "Modeling of the 2011 Japan tsunami: Lessons for near-field forecast." *Pure Appl. Geophys.*, 170(6–8), 1309–1331.

Yokota, Y., et al. (2011). "Joint inversion of strong motion, teleseismic, geodetic, and tsunami datasets for the rupture process of the 2011 Tohoku earthquake." *Geophys. Res. Lett.*, 38(7).